Atmospheric Environment 81 (2013) 660–670

Contents lists available at ScienceDirect

Atmospheric Environment

journal homepage: www.elsevier.com/locate/atmosenv

Atmospheric deposition of nitrogen and sulfur over southern Europe with focus on the Mediterranean and the Black Sea

U. Im [a,b,1], S. Christodoulaki [a,c], K. Violaki [a], P. Zarmpas [a], M. Kocak [d], N. Daskalakis [a,b], N. Mihalopoulos [a], M. Kanakidou [a,*]

[a] Environmental Chemical Processes Laboratory, Department of Chemistry, University of Crete, Voutes Campus, P.O. Box 2208, 71003 Heraklion, Greece
[b] Institute of Chemical Engineering Sciences, Foundation for Research and Technology Hellas (FORTH), Patras, Greece
[c] Institute of Oceanography, Hellenic Center for Marine Research, P.O. Box 2214, 71003 Heraklion, Crete, Greece
[d] Institute of Marine Sciences, Middle East Technical University, Erdemli, Mersin, Turkey

HIGHLIGHTS

- Atmospheric N and S depositions over Mediterranean and Black seas are simulated.
- N transported from upwind sources is deposited over the Mediterranean.
- Dry deposition dominates over wet deposition in Mediterranean and Black Sea.
- Atmospheric N inputs are comparable to N export in Black and W. Mediterranean seas.
- Atmospheric N input exceeds the N export in the East Mediterranean Sea.

ARTICLE INFO

Article history:
Received 24 February 2013
Received in revised form
17 September 2013
Accepted 21 September 2013

Keywords:
Atmospheric deposition
Nitrogen
Sulfur
Mediterranean Sea
Black Sea
WRF
CMAQ
Atmospheric chemistry and transport modeling

ABSTRACT

Atmospheric deposition provides significant amounts of nutrients to the continental and marine ecosystems. Using the mesoscale WRF/CMAQ modeling system, the nitrogen (N) and sulfur (S) atmospheric deposition fluxes over the Mediterranean and the Black seas and continental Europe are evaluated for the year 2008. The annual N and S deposition fluxes are calculated to be 4.89 Tg(N) yr^{-1} and 2.07 Tg(S) yr^{-1} over continental Europe, 0.92 Tg(N) yr^{-1} and 0.52 Tg(S) yr^{-1} over West Mediterranean, 1.10 Tg(N) yr^{-1} and 0.84 Tg(S) yr^{-1} over East Mediterranean and 0.36 Tg(N) yr^{-1} and 0.17 Tg(S) yr^{-1} over the Black Sea. Inorganic N deposition fluxes are calculated to be about 3 times higher than gaseous organic N deposition fluxes. Comparison to available observations associates the annual mean model estimates with about 40 ± 30% of uncertainty depending on location. Dry deposition dominates over wet deposition for both N and S in agreement with the observations. Results suggest that an important fraction of the N deposited over the Mediterranean basin can be attributed to transported N species while S deposition is dependent more on the local emissions. In Black Sea and West Mediterranean Sea waters the calculated atmospheric N inputs are comparable to the N export measured by sediment traps whereas in the East Mediterranean N input exceeds by a factor of about 5 the N export. Our simulations show that the critical N load of 1 g(N) m^{-2} yr^{-1} is exceeded over 84% of the European forested areas.

1. Introduction

Atmospheric deposition of nitrogen (N) and sulfur (S) species from both natural and anthropogenic sources lead either to benefits (fertilization) or drawbacks (acidification and accumulation of excess nutrients) for the ecosystems (Driscoll et al., 2003). With the advent of the Anthropocene the transfer of these species has increased over natural levels, modifying thus their biogeochemical cycles in both terrestrial and aquatic ecosystems (Galloway et al., 2008). First estimates indicate that the human-induced increase in atmospheric N deposition to the oceans may account globally for up to ~3% of the annual new oceanic primary productivity (Duce et al., 2008). Especially for semi-enclosed marine ecosystems such as the Mediterranean Sea, atmospheric deposition of N may account for up to 35–60% of new production (Christodoulaki et al., 2013). Furthermore, in the atmosphere, ozone (O_3) production is driven by nitrogen oxide (NO_x) availability and atmospheric acidity

* Corresponding author. Tel.: +30 2810 545033; fax: +30 2810 545166.
E-mail address: mariak@chemistry.uoc.gr (M. Kanakidou).
[1] Now at: Air and Climate Unit, Joint Research Centre, Ispra, Italy.

1352-2310/$ – see front matter © 2013 Elsevier Ltd. All rights reserved.
http://dx.doi.org/10.1016/j.atmosenv.2013.09.048

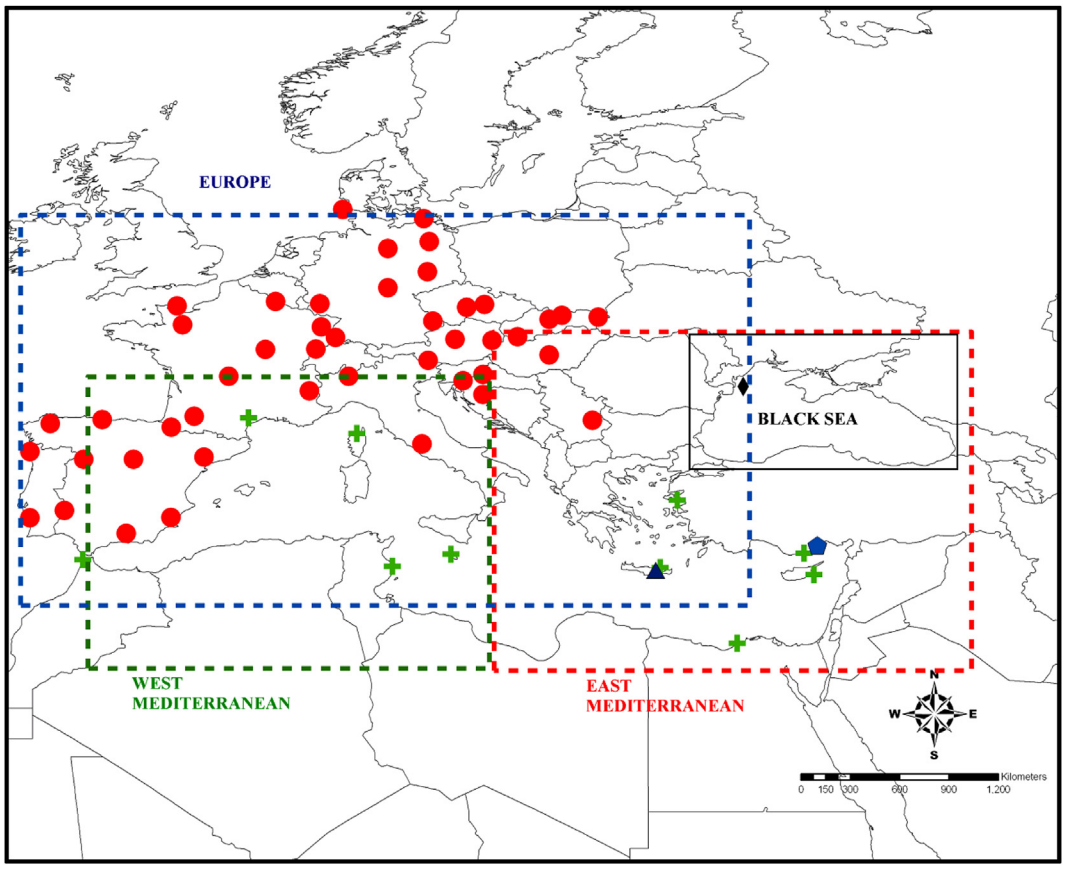

Fig. 1. The locations of the EMEP wet deposition stations (circles) and Finokalia station for dry deposition (triangle). Crosses represent monitoring stations in Markaki et al. (2010), diamond represents the monitoring station at Zmiinyi Island, Ukraine (Medinets and Medinets, 2012) and pentagon represents the monitoring station in Erdemli, Turkey (Kocak et al., 2010). The model domain extents from 18.98°N, 3.58°W to 49.82°N, 57.64°E. The EUROPE box represents Europe (from 29.95°N, 7.47°W to 54.98°N, 32.03°E), the East Mediterranean box represents East Mediterranean (from 41.31°N, 27.67°E to 46.37°N, 43.76°E) and the West Mediterranean box represents Western Mediterranean (from 27.60°N, 2.77°W to 45.17°N, 15.14°E). The Black Sea box extends from 41.31°N, 27.67°E to 46.37°N, 43.76°E.

is controlled by nitric acid (HNO_3) and sulfuric acid (H_2SO_4) formation (Seinfeld and Pandis, 2006). Thus, deposition of atmospheric N and S species impacts on atmospheric chemistry. There are different projections for the future levels of N and S deposition fluxes over Europe based on different emission scenarios in the literature that indicate control of the emissions of SO_2 and NO_x but not those of NH_3 (Dentener et al., 2006; Geels et al., 2012; Lamarque et al., 2013).

Monitoring of deposition, particularly dry deposition, is very challenging, especially over water bodies (Pryor et al., 2008), and can provide data of only limited geographical coverage (Fowler et al., 2009). Because deposition depends on surface characteristics (dry deposition) and precipitation rates (wet removal), significant interpolation errors can occur when deposition is to be evaluated over large areas based on observations. Atmospheric chemistry and transport models (CTMs) are unique tools to provide integrated view of the temporal and spatial variations of dry and wet deposition over local to global scales. CTMs can calculate critical loads in order to provide estimates of the environmental impact of deposition. They can use future emission estimates to assess environmental change and provide advice to policy makers. Such model output requires extensive evaluation by comparison to observed deposition fluxes (Flechard et al., 2011).

Simpson et al. (2006) European Monitoring and Evaluation Programme (EMEP) mesoscale modeling study calculated that dry deposition of reduced N species is the major contributor to total reactive N deposition in Central and southern Europe. Menegoz et al. (2009) global CTM simulations of sulfate ($SO_4^{=}$) compared with EMEP observations over Europe showed overestimations in surface atmospheric $SO_4^{=}$ levels that have been attributed to underestimated wet deposition.

Despite the importance of atmospheric deposition for ecosystems, there is a limited number of modeling studies dedicated to the evaluation of atmospheric deposition of N and S to the Mediterranean and the Black Seas (e.g. Markaki et al., 2010; references therein, Medinets and Medinets, 2012). The present mesoscale modeling study aims to fill this gap by performing, the first to our knowledge study of one full year mesoscale simulation of atmospheric deposition of N and S over Europe, with special focus on the Mediterranean and Black Sea.

2. Materials and methods

2.1. The modeling system

The Advanced Research Weather Research and Forecasting mesoscale meteorological model (WRF-ARW v3.1.1; Skamarock and Klemp, 2008) has been used to calculate the meteorological fields necessary to drive the Community Multiscale Air Quality (CMAQ) model, v4.7 (Byun and Schere, 2006). The model domain (Fig. 1) covers most of the Europe, North Africa and the Middle East (from 18.98°N, 3.58°W to 49.82°N, 57.64°E) on a 30 × 30 km horizontal resolution, extending up to ~16 km on 23 vertical levels. The initial and boundary meteorological conditions for the WRF model have

Table 1
Source-specific annual and seasonal domain-integrated emissions (annual emissions in Gg yr^{-1}; seasonal emissions in Gg $season^{-1}$).

Emissions (Gg $season^{-1}$ or Gg yr^{-1})		CO	NO_x[b]	SO_2	NH_3	NMVOC	PM10
Anthropogenic[a]	Winter	1.3E+04	4.8E+03	4.7E+03	3.5E+02	6.3E+03	1.0E+03
	Spring	9.8E+03	3.7E+03	2.7E+03	4.5E+02	5.2E+03	7.8E+02
	Summer	9.4E+03	4.3E+03	3.2E+03	9.2E+02	4.7E+03	6.9E+02
	Autumn	1.1E+04	4.6E+03	3.7E+03	4.0E+03	5.3E+03	1.0E+03
	Annual	4.3E+04	1.7E+04	1.4E+04	5.7E+03	2.1E+04	3.5E+03
Biogenic	Winter	6.5E−05	3.7E+01			1.9E+03	
	Spring	1.4E−02	1.3E+02			1.1E+04	
	Summer	1.2E−01	3.9E+02			4.1E+04	
	Autumn	5.9E−03	1.2E+02			9.3E+03	
	Annual	1.4E−01	6.8E+02			6.3E+04	
Dust	Winter						7.7E+04
	Spring						1.2E+05
	Summer						9.7E+04
	Autumn						6.5E+04
	Annual						3.6E+05
Biomass burning	Winter	1.1E+00	5.4E−02	7.3E−03	1.9E−02	5.5E−01	6.5E−02
	Spring	4.6E+00	2.3E−01	2.5E−02	8.3E−02	2.8E+00	2.2E−01
	Summer	2.9E+01	1.5E+00	1.2E−01	5.8E−01	2.2E+01	1.1E+00
	Autumn	9.7E+00	4.9E−01	4.1E−02	1.9E−01	7.3E+00	3.9E−01
	Annual	4.4E+01	2.2E+00	1.9E−01	8.7E−01	3.3E+01	1.8E+00

[a] Anthropogenic includes shipping, aviation, agricultural emissions and land anthropogenic emissions.
[b] NO_x ($NO + NO_2$) is assumed to be emitted by 90% as NO.

been provided by the National Centers for Environmental Prediction (NCEP) on a 1° horizontal and 6-h temporal resolution. The WRF and CMAQ configurations and precipitation parameterizations are given in Table S1 and discussed in the supplementary material (see also Im et al., 2013).

Monthly initial and boundary chemical conditions for the CMAQ model have been extracted from the global chemistry- Transport Model v.4 of the Environmental Chemical Processes Laboratory (TM4-ECPL) on a 3° × 2° spatial resolution and 34 vertical levels up to 0.1 hPa (~65 km; Myriokefalitakis et al., 2011). Both WRF and CMAQ models used a spin-up period of 20 days in December 2007 and the simulation period covered the year 2008 (366 days).

2.2. Deposition calculations

In CMAQ, dry deposition of particles is calculated by turbulent air motion and by direct gravitational sedimentation of large particles (Pleim et al., 2001), using the resistance model approach developed by Wesely and Hicks (1977). Dry deposition velocities of gases are calculated by the Meteorology–Chemistry Interface Processor (MCIP; Otte and Pleim, 2010) (see details in the supplementary material). The seasonal variations of model-calculated dry deposition velocities of gases of interest are provided in Table S2. Uncertainty in the simulations of dry deposition fluxes is large. Flechard et al. (2011) evaluated that differences in the representations of canopy characteristics of land use types, stomatal conductance, non-stomatal resistances, deposition velocities and exchange rates between models lead to high uncertainties in simulated dry deposition fluxes (up to a factor of 3 for gases and a factor of 10 for aerosols).

Wet deposition is calculated in the cloud module of CMAQ. Wet deposition is determined by the Henry's Law constant of the gaseous tracer or scavenging rate of the aerosol mode and component. CMAQ calculates the wet deposition by using an algorithm that allocates precipitation amounts to individual layers based on a normalized profile taking into account the non-convective precipitation rate, sum of hydrometers (rain, snow and graupel) and layer thickness to avoid excessive removing from thin layers and little from thick layers (Foley et al., 2010). Organic nitrogen (ON) is calculated as the sum of the gaseous peroxy acetyl nitrates (PAN) and organic nitrates (NTR) while inorganic nitrogen (IN) is derived as the sum of gas and aerosol species: nitrate (NO_3^-), ammonia (NH_3), ammonium (NH_4^+), HNO_3, N_2O_5, NO, NO_2 and HONO. Sulfur deposition flux is calculated as the sum of $SO_4^=$, H_2SO_4 and SO_2 deposition fluxes.

2.3. Emissions

The European anthropogenic emissions have been taken from the emission inventory of the French National Institute of Industrial Environment and Risks (INERIS: https://wiki.met.no/cityzen/page2/emissions) provided in the frame of the CityZen project, which is a re-gridded product of the 50 km × 50 km EMEP inventory (http://www.ceip.at/). These emissions include shipping, aviation, agricultural emissions and land anthropogenic emissions. Anthropogenic emissions from the remaining areas (i.e. North Africa and the Middle East) have been provided by the Climate change and Impact Research: the Mediterranean Environment (CIRCE) global emissions inventory (Pozzer et al., 2012). Details on natural emission calculations are given in the supplementary material.

The annual emissions from anthropogenic and natural sources of gaseous and particulate atmospheric constituents used in the model are given in Table 1. On annual basis, anthropogenic sources are the major contributors to the gaseous pollutants in the region whereas for particulate matter (PM), natural dust emissions are 2 orders of magnitude higher than anthropogenic emissions. The inorganic reactive N and S annual emission distributions are depicted in Fig. 2. The hot spot regions of London, Benelux, Po Valley, Istanbul, Athens and Cairo and the shipping routes, particularly in the Mediterranean Sea and along the west coast of Europe, clearly stand out. Source intensity of these areas may vary depending on the pollutant. As an example, Po Valley stands out as an important N source (Fig. 2a) in the region while this is not the case for S emissions (Fig. 2b). The annual and seasonal variations of N and S emissions over the studied regions are also given in Table 4.

2.4. Wet and dry deposition observations

EMEP (http://www.emep.int/) provides rain water concentrations of pollutants and precipitation rates, at background stations over Europe (Tørseth et al., 2012). Additional N and/or S deposition flux measurements over Europe are reported in literature (Morales-

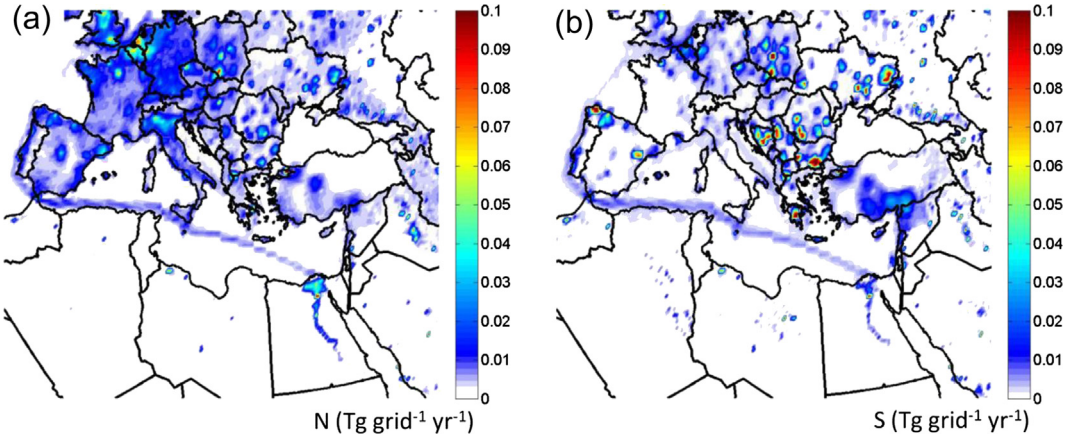

Fig. 2. (a) Nitrogen (NO_x, NH_3 and particulate nitrate) and (b) sulfur (SO_2 and particulate sulfate) emissions used in the model and integrated over the year 2008 (grid resolution is 30 km).

Baquero et al. (2006) for Sierra Nevada, Spain; Anatolaki and Tsitouridou (2007) for Thessaloniki, Greece; Violaki et al. (2010) for Crete, Greece and Markaki et al. (2010) for the Mediterranean basin). Erisman et al. (2005) documented that uncertainty in wet deposition measurements is high (up to 40%). Note that uncovered wet deposition collectors can have a positive bias in measured concentrations in precipitation due to dry deposition to the collector surface thus causing an artificial appearance of underestimation in modeled wet deposition. Such bias is expected to be more effective during summer. At Finokalia (FKL), an atmospheric monitoring station located at a central point in the East Mediterranean basin (35.20°N, 25.40°E, 250 m asl; Mihalopoulos et al., 1997) wet deposition measurements were made with wet-only collectors. Wet deposition fluxes are derived as the product of the precipitation amounts and the measured rain water concentrations of $SO_4^=$, NO_3^- and NH_4^+, provided by EMEP in the EBAS database (http://ebas.nilu.no). A total of 45 stations reported precipitation and rain water concentration data inside the studied region for 2008 (Fig. 1 and Table S3). The wet deposition fluxes are then integrated seasonally and annually. In addition, observed monthly dry deposition fluxes of $SO_4^=$, NO_3^- and NH_4^+ derived from observations (see details in the supplementary material) at FKL are used to evaluate the model performance on a seasonal and annual basis. FKL is now part of the EMEP and ACTRIS (Aerosols, Clouds, and Trace gases Research InfraStructure) networks. Soluble IN observations of bulk (wet and dry) atmospheric deposition fluxes (measured using a plate bulk deposition sampler, as the sum of NO_3^-, NH_4^+ and NO_2^-, this later being <0.2% of the total fluxes) at the Zmiinyi Island in the northwestern Black Sea in 2008 (Medinets and Medinets, 2012) have been also used for model evaluation.

The spatial coverage of the model evaluation has been increased by using deposition data from the region for years other than 2008. Annual and seasonal bulk deposition fluxes of soluble IN from Cap Spartel (Morocco), Mahdia (Tunisia), Gozo (Malta), Cavo Greco (Cyprus) and Akkuyu (Turkey) for the period 2001 to 2003 (Markaki et al., 2010) as well as dry (2006–2007) and wet (2006) deposition data of NO_3^- and NH_4^+ from Erdemli, a coastal site at southeastern Turkey (Kocak et al., 2010) have been also compared with the model results. Observed dry deposition fluxes were deduced from measured atmospheric levels of NO_3^- and NH_4^+ and dry deposition velocities reported by Kocak et al. (2010). Wet deposition fluxes are derived from rainwater concentrations and precipitation amounts.

The following commonly used statistical parameters have been calculated as benchmark for comparisons between model results and observations: Correlation coefficient (*r*), *BIAS*, normalized mean bias (*NMB*), root mean square error (*RMSE*), mean absolute gross error (*MAGE*), normalized mean error (*NME*) and index of agreement (*IOA*) (see definitions in the supplementary material). Only the model calculated deposition fluxes that correspond to the periods with observations have been used for the comparisons.

3. Results

3.1. Assessment of CMAQ performance to simulate atmospheric deposition

Atmospheric distributions of trace gases and aerosols simulated using the same WRF-CMAQ set up used here but focusing over the East Mediterranean have been evaluated by Im et al. (2011, 2012) and Im and Kanakidou (2012). A detailed evaluation of the atmospheric pollutant distributions derived by the CMAQ simulations used in the present study is presented by Im et al. (2013). Here we focus on evaluation of the model derived deposition fluxes by comparison to observationally derived data. Simulated deposition fluxes are affected by the emissions input and the model computed transport, chemistry and precipitation patterns. Therefore inaccuracies in all these deposition drivers cause differences between observations and models. In particular, uncertainties in the simulated precipitation and chemistry directly reflect in the calculated deposition fluxes. In some case such discrepancies can counterbalance and reduce the overall biases between observed and simulated deposition fluxes. Thus, hereafter we also provide an outlook of the ability of the model to simulate observed precipitation rates in the studied region.

3.1.1. Simulated precipitation

In this respect, simulated precipitation rates are compared with EMEP observations and the statistical evaluations of precipitation for all these stations are provided in Table 2. Precipitation (Fig. 3a) is underestimated by the model by about 12% on an annually-integrated basis (Table 2) with the largest underestimation (NMB = 20%) in fall and a slight overestimation (2%) in summer. The spatial distribution of the NME at these EMEP stations (Fig. 3b), reveals the largest NMEs over the Balkans and Italy and the smallest over Central Europe. Additional comparisons for the NitroEurope stations (Flechard et al., 2011) provided in the supplementary Figure S1 indicate that the model is able to capture the general pattern of precipitation rates but presents significant deficiency in

Table 2
Statistical comparison of annual and seasonal observed and modeled wet deposition fluxes at the EMEP stations (number of pairs = 44). Bias and MAGE are in μg m^{-2} per year or per season for wet deposition fluxes and mm per year or per season for precipitation amounts. NMB and NME are in percent.

		r^2	Bias	NMB	RMSE	IOA	MAGE	NME
	NH_4^+	0.3	−198	−53	262	0.6	201	54
	NO_3^-	0.4	−47	−17	146	0.8	110	39
	$NH_4^+ + NO_3^-$	0.4	−165	−47	226	0.7	170	48
	$SO_4^=$	0.2	−125	−36	267	0.6	172	46
	Precipitation	0.5	−116	−12	417	0.8	318	33
Winter	NH_4^+	0.1	−37	−68	51	0.5	38	70
	NO_3^-	0.1	−9	−19	37	0.6	27	54
	$NH_4^+ + NO_3^-$	0.1	−31	−58	45	0.5	35	65
	$SO_4^=$	0.2	−28	−41	55	0.6	38	56
	Precipitation	0.2	−23	−11	118	0.7	88	41
Spring	NH_4^+	0.2	−106	−80	142	0.4	106	80
	NO_3^-	0.5	−21	−23	52	0.8	38	42
	$NH_4^+ + NO_3^-$	0.3	−87	−71	118	0.5	88	71
	$SO_4^=$	0.4	−37	−34	68	0.7	53	47
	Precipitation	0.6	−29	−10	120	0.9	90	31
Summer	NH_4^+	0.3	−80	−67	104	0.5	81	67
	NO_3^-	0.4	−16	−21	48	0.8	34	46
	$NH_4^+ + NO^-$	0.3	−66	−60	87	0.6	67	60
	$SO_4^=$	0.4	−12	−13	53	0.8	44	48
	Precipitation	0.3	5	2	204	0.6	127	52
Fall	NH_4^+	0.2	33	53	72	0.5	52	82
	NO_3^-	0.4	13	22	42	0.7	30	53
	$NH_4^+ + NO_3^-$	0.3	29	47	65	0.6	46	75
	$SO_4^=$	0.3	−19	−23	58	0.7	41	49
	Precipitation	0.6	−46	−20	102	0.9	80	34

capturing the extreme events. Furthermore, the overestimate of precipitation during summer might be due to the convective precipitation simulations. Thus, although our model resolution is high compared to larger-scale models, the comparison of modeled precipitation to observations at specific stations remains a challenge due to the high temporal and spatial variability of precipitation events (Matthias et al., 2008; Appel et al., 2011).

3.1.2. Simulated atmospheric deposition

Fig. 3c–e depict the scatter diagrams of the observed and simulated annual precipitation and $SO_4^=$, NO_3^- and NH_4^+ wet deposition fluxes while Table 2 provides the statistical information on annual and seasonal basis. Pollutant annual wet deposition fluxes are underestimated by 36% for $SO_4^=$, by 17% for NO_3^- and by 49% for NH_4^+. Overall, the simulated annual wet deposition flux of N (sum of NO_3^- and NH_4^+) underestimates by 47% the observationally derived flux. On a seasonal basis, the model shows similar performances (Table 2). With the exception of fall, wet deposition fluxes of NO_3^- and NH_4^+ are underestimated in all other seasons. In fall, the fluxes overestimate by the model is attributed to that in the N sources (primary, secondary or long range transport), since precipitation fluxes are largely underestimated. Biases in observations of wet deposition (Section 2.4) could also contribute to these discrepancies between model and observations. For the other seasons, relatively smaller underestimations of precipitation rates compared to the wet deposition fluxes suggest underestimations of sources, particularly in spring, leading to the largest underestimation of IN deposition flux in spring.

Annual dry deposition fluxes at FKL are largely underestimated by the model for $SO_4^=$ and NH_4^+ and for total N by 30%, with larger seasonal biases (Table 3a). Keeping in mind the large uncertainties in dry deposition estimates discussed in Section 2.2 this comparison is satisfactory. On the opposite, although annual precipitation rate (313 mm) compares very well with the observed rate (~300 mm), the simulated bulk and wet deposition fluxes of the sum of NO_3^- and NH_4^+ over the Zmiinyi Island in Black Sea highly overestimate the observations of the specific year by a factor of ~2 while they lie in the range of the 6 years period fluxes (Table 3a). This large difference between model and observations is due to NO_3^- which according to the model contributes by 87% to the IN wet deposition while Medinets and Medinets (2012) reported a NO_3^- contribution of about 18%. Recent measurements at two other locations of the Black Sea (Varna, Bulgaria, and Sinop, Turkey; Mihalopoulos et al., unpublished work 2013) show NO_3^- as the main

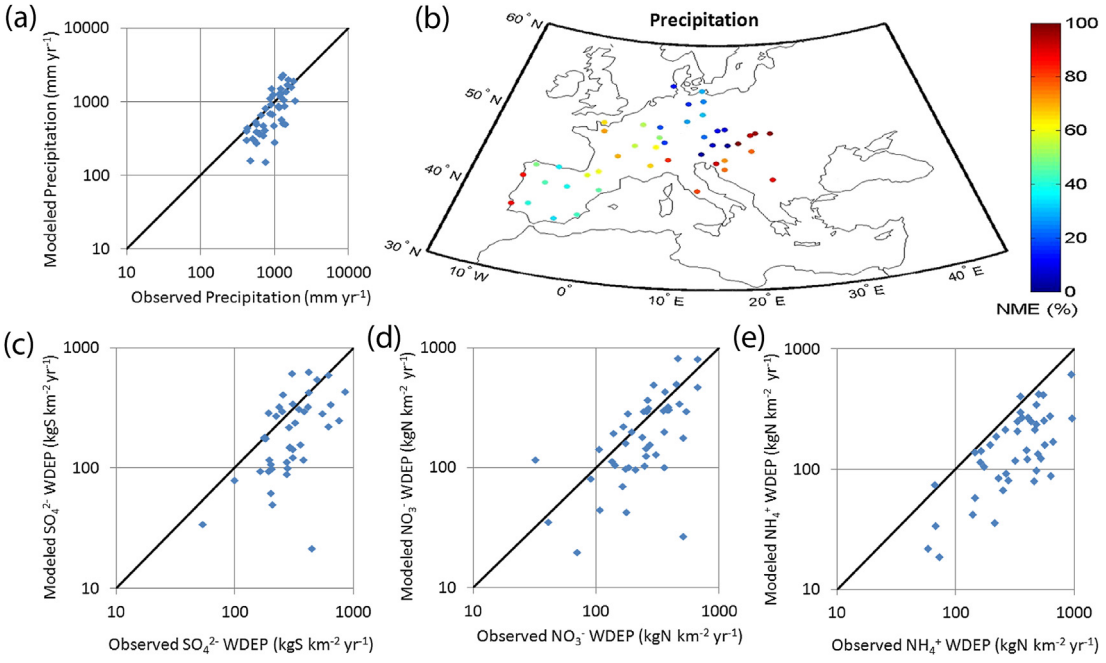

Fig. 3. (a) Scatter diagram of modeled and observed annual precipitation (b) spatial distribution over Europe of the normalized mean error of the simulated precipitation (see Appendix for definition); and Scatter diagram of modeled and observed annual wet deposition fluxes (WDEP) of (c) $SO_4^=$, (d) NO_3^- and (e) NH_4^+ at the EMEP stations. Each diamond corresponds to the annual flux at each EMEP station depicted in Fig. 1 and Table S3.

Table 3a
Comparison of simulated deposition fluxes for the year 2008 (Mod.) with observations (Obs.). Units are in g(N) m^{-2} yr^{-1} or g(S) m^{-2} yr^{-1}.

	NO_3^-		NH_4^+		$NO_3^- + NH_4^+$		$SO_2 + SO_4^=$		References
	Obs.	Mod.	Obs.	Mod.	Obs.	Mod.	Obs.	Mod.	
Finokalia, Crete (2008)[a]	0.09	0.07	0.04	<0.01	0.13	0.07	0.22	0.05	Mihalopoulos et al. unpublished data
Zmiinyi Island, Ukraine (2008)					0.27 ± 0.05	0.53			Medinets and
(2004–2010)					0.69 ± 0.07				Medinets (2012)
Erdemli, Turkey (2006–07)	1.29	1.30	0.56	0.21	1.85	1.51			Kocak et al. (2010)
Akkuyu, Turkey (2001–03)[b]					0.42	0.86			Markaki et al. (2010)
Cap Spartel, Morocco (2001–03)[b]					0.39	0.87			Markaki et al. (2010)
Cavo Greco, Cyprus (2001–03) [b]					0.67	0.99			Markaki et al. (2010)
Mahdia, Tunisia (2001–03)[b]					0.25	0.79			Markaki et al. (2010)

[a] Only dry deposition fluxes.
[b] N is calculated as the sum of N in NO_3^-, NH_4^+, NH_3, HNO_3 and N_2O_5.

contributor of IN deposition, indicating significant spatial variability within the area. At the Erdemli site, annual total deposition flux of NO_3^- agrees well with the reported value while NH_4^+ is underestimated by 38% (Kocak et al., 2010). Simulated annual N deposition fluxes in the Mediterranean region for 2008 compare reasonably well with observations in 2001–2003 by Markaki et al. (2010), with overestimation by 50%–100% on annual basis (Table 3a) with the exception of Mahdia, Tunisia. The model simulates larger contribution of dry deposition to total IN deposition fluxes (67%) compared to wet deposition (33%), in agreement with Markaki et al. (2010) who reported 60% and 40% contributions of dry and wet deposition, respectively. In general, dry deposition fluxes are calculated to be higher than wet deposition fluxes both for N and S species in all studied regions (Table 4).

3.2. Nitrogen and sulfur deposition

Annual total (wet and dry) deposition fluxes of N and S are calculated for the continental Europe, the Mediterranean basin and the Black Sea (see Fig. 1 for the area definitions). The Mediterranean basin is further divided into West Mediterranean and East Mediterranean. These calculated total annual deposition fluxes are depicted in Fig. 4. Table 4 summarizes the simulated annual and seasonal wet and dry deposition fluxes of N and S while ON and IN deposition fluxes over these regions are provided in Table S4 in the supplementary material. Regional estimates of deposition fluxes compare well with earlier studies (Table 3b). Because of the interest of atmospheric deposition over the Black Sea for regional studies, atmospheric deposition over the Black Sea has been also computed separately, although the Black Sea is also part of the East Mediterranean domain.

The simulated total N and S deposition fluxes over the Black Sea of 0.36 Tg(N) yr^{-1} and 0.17 Tg(S) yr^{-1} (Fig. 4a and b) are comparable with the 0.20 Tg(N) yr^{-1} and 0.26 Tg(S) yr^{-1} reported by EMEP (2010). Deposition is generally higher over the coastal regions due to the vicinity of emissions. Table 4 shows that for both S and N total deposition fluxes, East Mediterranean and the Black Sea together experience 1.5–2 times higher values than West Mediterranean. Total N deposition fluxes for the Mediterranean Sea is about twice the estimated by EMEP (2010), while the here computed S deposition flux is comparable with the EMEP (2010) estimates. The calculated continental Europe annual N and S deposition fluxes are shown in Fig. 4e and f. When both land and sea are considered, N deposition agrees well with the earlier estimates over Europe that span between 5.6 and 12.3 Tg(N) yr^{-1} (Table 3b), while total deposition flux of S remains by at least 60% lower than the earlier estimates that span between 6.4 and 11.2 Tg(S) yr^{-1}. Lamarque et al. (2013) ensemble modeling report a mean deposition flux rates of 1.06 g(N) m^{-2} yr^{-1} and 1.08 g(S) m^{-2} yr^{-1} for Central Europe very close to the 0.97 g(N) m^{-2} yr^{-1} but double the 0.49 g(S) m^{-2} yr^{-1} here calculated for the European model domain. Differences can be attributed to differences in domain definitions regarding Europe and in model resolutions. Boundary conditions are also important for long-lived pollutants, particularly considering the importance of inflow to the Mediterranean region, as shown by Im and Kanakidou (2012).

Annual wet deposition flux of TN over West Mediterranean is slightly higher than over East Mediterranean Sea while S wet deposition flux over the east basin is 50% higher than over the west basin. Simulations show ~40% higher precipitation over the West Mediterranean (~491 mm yr^{-1}) than the East Mediterranean. Both S and N emissions show an opposite to precipitation pattern, being 50% higher for N and almost 4 times higher for S over the East than the West Mediterranean. The simulations show that annual N deposition fluxes over East Mediterranean are equivalent to 130% of the N emissions from the same area, suggesting transported N to the region that is deposited here. On the other hand, annual S deposition over East Mediterranean is equivalent to 72% of the S annual emissions from the same area, suggesting that the S is exported to downwind regions. Higher ratios are calculated for the West Mediterranean (179% and 96% for N and S respectively), suggesting larger regional and local emission impacts over the West than the East Mediterranean. Over the continental Europe, total N and S deposition is calculated to be equivalent to 83% and 76% of the European N and S emissions, respectively.

Table S4 shows that both computed wet and dry deposition fluxes of IN are higher than ON. Over continental Europe, IN deposition flux is almost a factor of 3 higher than ON. Over the Black Sea, ON and IN dry deposition fluxes are comparable in agreement with Medinets and Medinets (2012), while over the East and West Mediterranean Sea, dry deposition fluxes of IN are larger up to a factor of 2 than ON, in agreement with Markaki et al. (2010). Those comparisons have to be seen with caution since in the present study, we do not account for ON present in the particulate form (Kanakidou et al., 2012 and the references therein). The here neglected contribution of particulate ON to atmospheric deposition of ON has been estimated to be ~70%, globally (Kanakidou et al., 2012).

The spatial distributions of N and S deposition fluxes over Europe reflect their emission distributions (Fig. 2) and their short term outflow downwind source regions, particularly over the Po Valley, Benelux and Northern France. The model estimates that over continental Europe, 19% of total N is deposited over forested regions, with 84% of these regions receiving fluxes larger than the critical nitrogen load of 1 g(N) m^{-2} yr^{-1}. This exceedance is calculated for over most of the continental Europe except for Spain and Portugal, with larger exceedances over north Western Europe, particularly over Benelux, and also over Po Valley (Fig. 4e). It

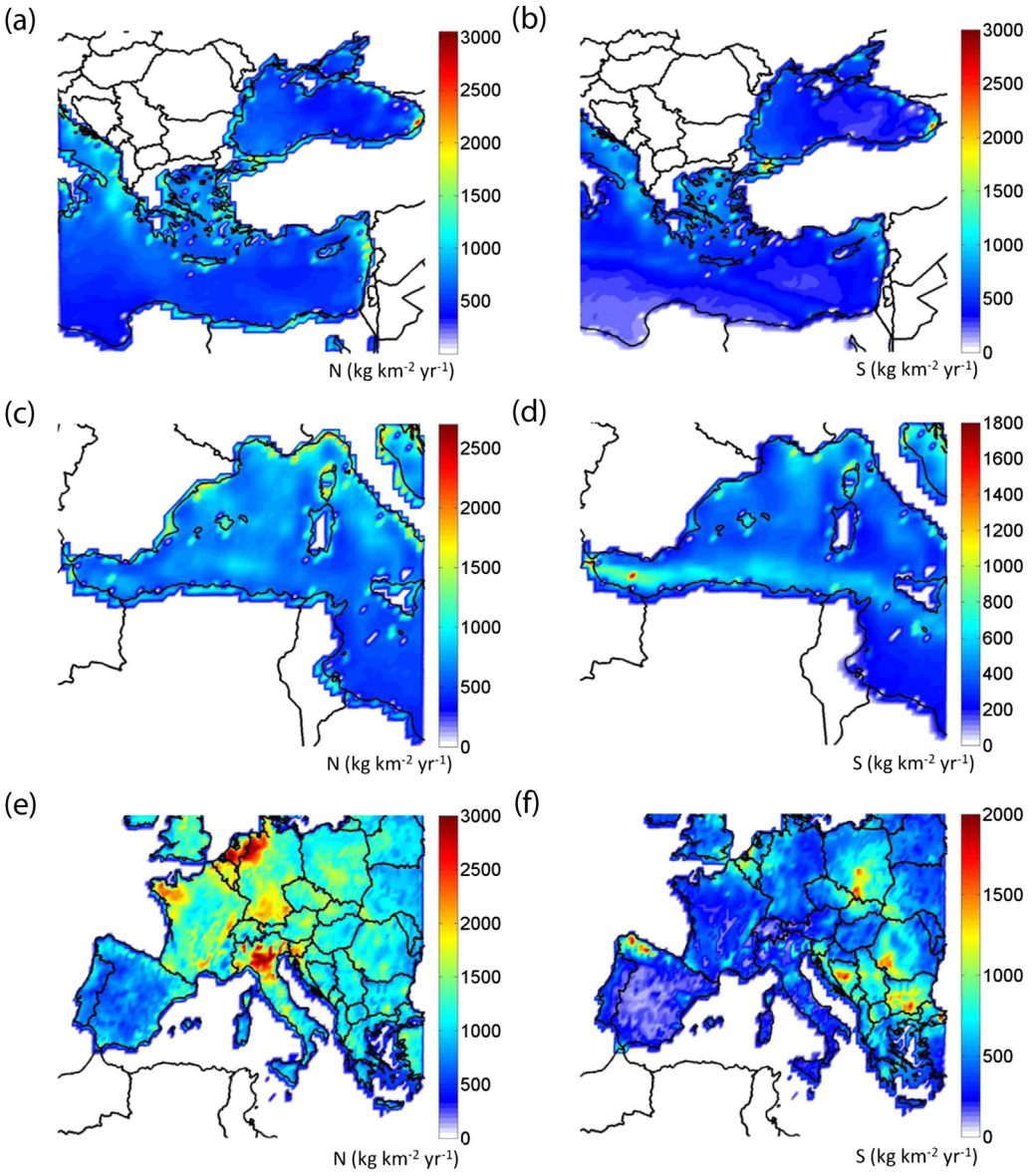

Fig. 4. Annually integrated atmospheric N (kg (N) km^{-2} yr^{-1}; left panels) and S (kg (S) km^{-2} yr^{-1}; right panels) deposition fluxes over East Mediterranean including Black Sea (a,b), West Mediterranean (c,d) and continental Europe (e,f). Nitrogen is calculated as the sum of PAN, NTR, NO_3^-, NH_3, NH_4^+, HNO_3, N_2O_5, NO, NO_2 and HONO. Sulfur is calculated as the sum of aerosol nss-$SO_4^=$, H_2SO_4 and SO_2.

indicates an imbalance in the nutrient cycling that leads to a change in the ecosystem diversity (Bobbink et al., 1998; UN-ECE, 2010). Our results agree with Dentener et al. (2006) who using 23 CTMs calculated that 30% and 80% of vegetation in western and Eastern Europe, respectively, are affected by deposition over the critical N load threshold.

3.3. Seasonality of nitrogen and sulfur deposition over the Mediterranean basin and Europe

The simulated seasonal variations of wet and dry deposition fluxes of TN (ON and IN) and S are depicted in Fig. 5 for each focus area (values also in Table 4 and S4). Over Black Sea, both dry and wet deposition fluxes of TN maximize in fall (0.08 and 0.05 Tg(N) $season^{-1}$, respectively) and minimize in spring, following the N emissions. Regarding S deposition over Black Sea, the maximum dry deposition is calculated in winter and the minimum in summer, following the S emissions. Wet deposition fluxes of S over the area maximize in fall and winter and minimize summer and spring following precipitation.

Over the East Mediterranean (Fig. 5a and b and Table 4), dry deposition fluxes of TN maximize in fall and minimize in spring while wet deposition fluxes of TN are less than half the dry deposition maximizing in winter and minimizing in summer. Similarly, in this area the largest and smallest wet deposition fluxes of S are calculated in winter and in summer, respectively, with a maximum-to-minimum ratio of 10, while dry deposition fluxes of S maximize in winter and minimize in spring with a maximum-to-minimum ratio of about 2. The West Mediterranean shows a similar seasonal pattern in deposition fluxes with Black Sea that differs from the East Mediterranean in the seasonal pattern of the wet deposition flux that maximizes in fall due to 2 times higher precipitation rate over the West than the East Mediterranean.

Over the continental Europe (Fig. 5c and d and Table 4), dry deposition fluxes of TN maximize in fall (1.74 Tg(N) $season^{-1}$) and minimize in winter (0.58 Tg(N) $season^{-1}$), following the seasonal

Table 3b
Comparison of simulated total annual deposition fluxes with other modeling studies in the literature. Units are in Tg(N) yr^{-1} and Tg(S) yr^{-1} for Nitrogen and Sulfur deposition fluxes over Black Sea, Mediterranean Sea and Europe. (*) Significant differences exist in the definition of the European domain and the year of the flux estimate. N deposition refers to the sum of deposition fluxes of all N-containing species in the model. S deposition refers to SO_2 and $SO_4^=$ deposition fluxes.

Region*	Year	N deposition	S deposition	References
Black Sea	2005	0.21		Bartnicki and Fagerli (2008)
	2008	0.20	0.26	EMEP (2010)
	2008	0.36	0.17	This study (sea only)
Mediterranean	2005	0.97		Bartnicki and Fagerli (2008)
	2008	0.94	1.09	EMEP (2010)
	2008	2.02	1.36	This study (sea only)
Europe	1978–94	8.4–11.2		Holland et al. (2005)
	2006	8.1	6.4	Aan de Brugh et al. (2011)
	2005–08	7.4	7.5	Pozzer et al. (2012)
	2000	5.6	8.6	Lamarque et al. (2013)
	2008	12.3	11.2	EMEP (2010)
	2008	7.7	3.9	This study (land and sea)

pattern of N emissions. Same seasonal variation is calculated for the wet deposition flux of total N with the maximum in fall (0.29 Tg(N) $season^{-1}$) and minimum in winter (0.11 Tg(N) $season^{-1}$) due to the emissions. Regarding S, the dry deposition flux maximizes in winter (0.59 Tg(S) $season^{-1}$) and minimizes in summer (0.26 Tg(S) $season^{-1}$) following S emissions. Contrary to the seasonality in S emissions and precipitation, wet deposition flux of S over the continental Europe is calculated to be largest in spring and summer. However, when both land and sea are considered in the defined region (Fig. 1), maximum and minimum wet deposition fluxes of S are calculated in fall and spring, respectively, following the emission and precipitation patterns, suggesting transport of land emissions over the sea. The model estimates a very low seasonal variability of total N (TN = IN + ON) deposition over the European forests (18%–20%).

Deposition-to-emission equivalent ratios for N and S for each focus area indicate that largest contribution from medium and long-range transport occurs during transition seasons. Similar to the annual equivalent ratios, this ratio is larger for N compared to S for all seasons. For the Mediterranean, the ratios for N are larger than 1 while for S, they are generally lower than 1, suggesting that transport from upwind locations is an important source of N in the Mediterranean. However, it should be noted that these ratios are subject to changes depending on the definitions of the areas and should be treated carefully. Over continental Europe, these ratios are lower than 1 as expected.

3.4. Significance of atmospheric N input to the Mediterranean and Black Sea

The relative importance of these simulated atmospheric N inputs to the Mediterranean and the Black Seas, is shown by comparison with the corresponding riverine N inputs to these seas, estimated for 1998 by Ludwig et al. (2009). A very small fraction of these riverine inputs also comes from the atmosphere. Simulated atmospheric N deposition (2.02 Tg(N) yr^{-1}) to the Mediterranean Sea is higher than the riverine inputs (1.08 Tg(N) yr^{-1}) by almost a factor of two. The atmospheric N deposition is calculated to be higher than the riverine inputs reported by Ludwig et al. (2009) (0.71 and 0.36 Tg(N) yr^{-1}, for the East and West Mediterranean). On the opposite in the Black Sea the riverine N input (1.12 Tg(N) yr^{-1}) is 3 times higher than the atmospheric deposition (0.36 Tg(N) yr^{-1}), although the here calculated atmospheric N deposition agrees with experimentally derived estimates.

Simulated atmospheric N deposition over the Mediterranean Sea (2.02 Tg(N) yr^{-1}) is within the range of the experimentally

Table 4
Simulated annual and seasonal dry and wet deposition fluxes of nitrogen and sulfur, and precipitation. N and S emissions used as input to CMAQ model. Data are reported for Black Sea (BS), East (EM) and West Mediterranean (WM) seas, continental Europe (EUR) and the entire simulation domain (Dom). See also Fig. 1 for area definitions. The parentheses show the total deposition over land + sea within the specified regions. For the Black Sea area only the sea surface is considered. Units are Tg(N) yr^{-1}, Tg(S) yr^{-1} and mm yr^{-1} or Tg(N) $season^{-1}$, Tg(S) $season^{-1}$ and mm $season^{-1}$.

		Nitrogen deposition (Tg(N) $period^{-1}$)			Sulfur deposition (Tg(S) $period^{-1}$)			Precipitation (mm $period^{-1}$)	Nitrogen emis. (Tg(N) $period^{-1}$)	Sulfur emis. (Tg(S) $period^{-1}$)
		Dry	Wet	Total	Dry	Wet	Total			
Annual	BS	0.23	0.12	0.36	0.16	<0.01	0.17	415	0.52	0.4
	EM	0.81 (2.88)	0.29 (0.85)	1.10 (3.73)	0.52 (1.37)	0.32 (0.70)	0.84 (2.07)	349 (405)	2.88	2.88
	WM	0.60 (2.80)	0.32 (0.65)	0.92 (3.45)	0.33 (0.48)	0.19 (0.33)	0.52 (0.81)	491 (384)	1.93	0.84
	EUR	4.14 (5.65)	0.75 (2.03)	4.89 (7.68)	1.59 (2.51)	0.49 (1.37)	2.07 (3.88)	504 (555)	9.26	5.08
	Dom	17.92	2.89	20.82	3.81	1.98	5.79	328	13.05	7.76
Winter	BS	0.05	0.03	0.08	0.07	0.02	0.09	138	0.09	0.12
	EM	0.20 (0.52)	0.12 (0.22)	0.32 (0.74)	0.21 (0.53)	0.11 (0.19)	0.32 (0.72)	174 (146)	0.55	0.89
	WM	0.13 (0.40)	0.08 (0.13)	0.21 (0.54)	0.11 (0.15)	0.06 (0.09)	0.16 (0.23)	181 (116)	0.39	0.23
	EUR	0.58 (0.90)	0.11 (0.39)	0.69 (1.29)	0.59 (0.90)	0.08 (0.32)	0.67 (1.22)	188 (159)	1.8	1.55
	Dom	3.53	0.57	4.1	1.34	0.44	1.78	104	4.78	4.8
Spring	BS	0.04	0.02	0.06	0.03	0.02	0.05	56	0.08	0.1
	EM	0.15 (0.60)	0.04 (0.19)	0.19 (0.78)	0.09 (0.29)	0.04 (0.18)	0.13 (0.47)	42 (84)	0.46	0.7
	WM	0.11 (0.81)	0.05 (0.13)	0.17 (0.94)	0.07 (0.11)	0.04 (0.08)	0.11 (0.19)	87 (92)	0.28	0.18
	EUR	0.70 (1.03)	0.19 (0.43)	0.89 (1.46)	0.36 (0.56)	0.15 (0.37)	0.51 (0.93)	106 (141)	1.42	1.18
	Dom	4.62	0.65	5.27	0.86	0.54	1.4	82	4.74	3.89
Summer	BS	0.06	0.02	0.08	0.02	0.02	0.04	61	0.16	0.08
	EM	0.20 (0.82)	0.01 (0.11)	0.21 (0.93)	0.09 (0.23)	0.01 (0.13)	0.10 (0.36)	22 (66)	0.64	0.6
	WM	0.14 (0.87)	0.02 (0.08)	0.16 (0.95)	0.06 (0.10)	0.01 (0.04)	0.07 (0.14)	15 (35)	0.45	0.21
	EUR	1.13 (1.53)	0.16 (0.36)	1.29 (1.89)	0.26 (0.43)	0.15 (0.28)	0.41 (0.72)	47 (98)	2.06	1.11
	Dom	4.79	0.5	5.29	0.68	0.42	1.1	64	5.44	3.3
Fall	BS	0.08	0.05	0.13	0.04	0.03	0.08	160	0.18	0.1
	EM	0.27 (0.94)	0.12 (0.33)	0.38 (1.28)	0.13 (0.33)	0.07 (0.20)	0.19 (0.52)	114 (115)	1.22	0.69
	WM	0.21 (0.71)	0.17 (0.31)	0.38 (1.02)	0.09 (0.12)	0.08 (0.13)	0.17 (0.25)	209 (143)	0.8	0.22
	EUR	1.74 (2.19)	0.29 (0.85)	2.02 (3.04)	0.38 (0.61)	0.12 (0.40)	0.49 (1.02)	165 (160)	3.97	1.24
	Dom	4.98	1.17	6.16	0.93	0.58	1.51	98	11.1	3.62

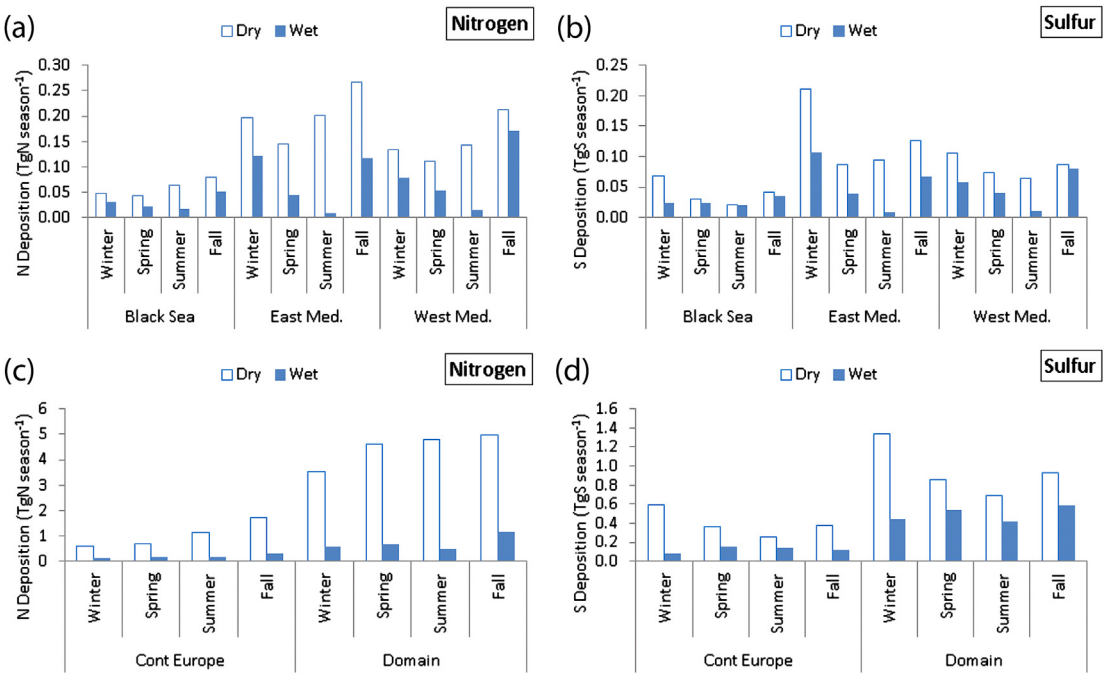

Fig. 5. Seasonal variation of simulated dry and wet deposition of N (sum of PAN, NTR, NO_3^-, NH_3, NH_4^+, HNO_3, N_2O_5, NO, NO_2 and HONO) and S (sum of nss-$SO_4^=$, H_2SO_4 and SO_2) over a,b) Black Sea and East and West Mediterranean Sea and c,d) continental Europe and the entire model domain (See Fig. 1 for domain and area definitions). Note difference in scales.

derived atmospheric deposition estimates of 0.27–2.06 Tg(N) yr^{-1} by Krom et al. (2004). Results show that atmospheric N input to the Mediterranean Sea is significant when compared to other sources such as intrusion of Atlantic surface water (0.79–1.89 Tg(N) yr^{-1}), rivers (1.08–1.20 Tg(N) yr^{-1}), groundwater (0.25 Tg(N) yr^{-1}) and point sources (0.27 Tg(N) yr^{-1}). Note however that riverine inputs are largely confined close to the land and thus atmospheric deposition is expected to be the main external to the ocean source of nutrients in the open sea.

The potential role of atmospheric N deposition on marine productivity can be investigated by comparing the calculated fluxes with new primary production. Due to the absence of continuous and long-term measurements of new production, sediment trap data can be a good proxy of new production. Assuming all deposited N is converted to biomass based on the Redfield stoichiometry (C:N ratio of 106:16, Redfield, 1934), the new production potentially sustained by the atmospheric deposition fluxes is estimated.

For Black Sea, the calculated atmospheric deposition of N can sustain an external carbon input of 2.4 Tg-C yr^{-1} that can counterbalance the outflux to the sediments of 1.6 Tg-C yr^{-1} derived from sediment traps measurements in the open Black Sea water by Theodosi et al. (2013). These results support an important role of atmospheric deposition for the open waters of the Black Sea. Similar approach can be applied for both the West and East Mediterranean basin. For the East Mediterranean the calculated atmospheric N deposition flux of 0.8 g(N) m^{-2} yr^{-1} is a factor of about 5 higher than the N export measured in sediments traps by Kouvarakis et al. (2001). Therefore, atmosphere can provide more than enough of the N required for phytoplanktonic development in this area, contributing to over-nutrification. The excess of N accumulates then in the water column and could explain the anomalous N/P ratio observed in the Eastern Mediterranean (Christodoulaki et al., 2013). For the West Mediterranean the role of N deposition is calculated to be smaller compared to the eastern basin but still significant. Indeed the atmospheric deposition of 0.9 Tg(N) yr^{-1} can sustain and new production of 5.2 Tg-C yr^{-1}, or 13 mg-C $m^{-2}d^{-1}$, which is within the range of the values reported by Ternon et al. (2010) at the Dyfamed site for a 4 year period. Again these results clearly indicate the predominant role of atmospheric deposition for the entire Mediterranean.

4. Conclusions

The distributions of annual (2008) and seasonal N and S deposition fluxes over Europe are simulated using a mesoscale WRF/CMAQ model system, separating the Black Sea from the West and East Mediterranean Seas, and the continental Europe. While regional deposition fluxes estimates lie within the range of earlier estimates, the model underestimates the deposition fluxes at individual monitoring sites by 10–80% depending on species, season and location. The largest differences are calculated for the wet deposition flux of NH_4^+, leading to discrepancies in the total nitrogen deposition. Annual precipitation, on the other hand, is underestimated only by 10–20% (although locally higher deviations from observations are found), suggesting the differences in observed and simulated deposition fluxes can be largely attributed to atmospheric sources (emissions, chemical production and transport). Note that precipitation scavenging is recognized as a major uncertainty in model simulations (Lamarque et al., 2013; Huneeus et al., 2011). The model generally underestimated total N deposition fluxes over the Mediterranean basin, with larger underestimations in organic compared to inorganic nitrogen. Overall comparisons of model results with observations show an average of 40 ± 30% underestimation on annual basis.

Despite the above discussed significant uncertainties in deposition calculations, the results show that dry deposition is more important than wet deposition in all focus areas and all seasons for both N and S deposition. East Mediterranean basin is calculated to receive more deposition than the West basin although it rains more in the West basin. Thus, differences in the deposition fluxes are attributed to differences in the emission patterns and physicochemical transformation between the two regions. Dry deposition fluxes of N are calculated to be largest in all studied regions during

fall while sulfur deposition maximizes in winter. On the other hand, wet deposition following the seasonal variation in precipitation, minimizing in summer and maximizing in fall. Annually, the Mediterranean Sea receives 2.02 Tg(N) yr^{-1} nitrogen and 1.36 Tg(S) yr^{-1} sulfur deposition while the Black Sea receives 0.36 Tg(N) yr^{-1} and 0.17 Tg(S) yr^{-1} nitrogen and sulfur, respectively. Continental Europe receives 4.89 Tg(N) yr^{-1} and 2.07 Tg(S) yr^{-1} nitrogen and sulfur deposition, respectively. Our model results compare well with previous model studies over Europe, particularly for nitrogen.

The results show that on annual basis, total deposition fluxes of nitrogen and sulfur are equivalent to more than 70% of the regional emissions in the areas of discussion. Simulations also suggest that a significant amount of the N deposition is transported N species to the Mediterranean basin while S deposition depends more on local emissions on annual and seasonal basis. Over most of the continental Europe, the critical for the ecosystems nitrogen deposition load of 1 g(N) m^{-2} yr^{-1} is exceeded, in particular, in 84% of the European forested areas (Scandinavian forests are not included in our study area). Comparisons with riverine N inputs to the Mediterranean and Black Seas suggest that atmospheric deposition is an important contributor to the nutrients external input in these marine ecosystems. Our results clearly indicate the predominant role of atmospheric deposition for the open Mediterranean and Black Sea waters.

Acknowledgements

This work has been performed in the frame of the European Union Seventh Framework Programme project PERSEUS (# 287600) and CityZen (# 212095). Support by ECLIPSE (FP7 # 282688) (UI) and ADAMANT (NSRF, 2007–2013) (SC) is acknowledged. G. Siour (LISA/IPSL/INERIS), B. Bessagnet (INERIS), U. Doering (Oko-Institute) and J. van Aardenene (EEA) are acknowledged for providing emission inventories and K. Markakis (LMD) for merging them for the mesoscale simulations. We thank the anonymous reviewer's for their pertinent comments.

Appendix A. Supplementary data

Supplementary data related to this article can be found at http://dx.doi.org/10.1016/j.atmosenv.2013.09.048.

References

Aan de Brugh, J.M.J., Schaap, M., Vignati, E., Dentener, F., Kahnert, M., Sofiev, M., Huijnen, V., Krol, M.C., 2011. The European aerosol budget in 2006. Atmos. Chem. Phys. 11, 1117–1139.

Anatolaki, Ch., Tsitouridou, R., 2007. Atmospheric deposition of nitrogen, sulfur and chlorine in Thessaloniki, Greece. Atmos. Res. 85, 413–428.

Appel, K.W., Foley, K.M., Bash, J.O., Pinder, R.W., Dennis, R.L., Allen, D.J., Pickering, K., 2011. A multi-resolution assessment of the Community Multiscale Air Quality (CMAQ) model v4.7 wet deposition estimates for 2002–2006. Geosci. Model Dev. 4, 357–371.

Bartnicki, J., Fagerli, H., 2008. Airborne load of nitrogen to European seas. Ecol. Chem. Eng. S-Chem. I Inzynieria Ekol. S 15, 297–313.

Bobbink, R., Hornung, M., Roelofs, J.M., 1998. The effects of airborne pollutants on species diversity in natural and semi-natural European vegetation. J. Ecol. 86, 717–738.

Byun, D., Schere, K.L., 2006. Review of the governing equations, computational algorithms, and other components of the models-3 Community Multiscale Air Quality (CMAQ) modeling system. Appl. Mech. Rev. 59, 51–77.

Christodoulaki, S., Petihakis, G., Kanakidou, M., Mihalopoulos, N., Tsiaras, K., Triantafyllou, G., 2013. Atmospheric deposition in the Eastern Mediterranean, a driving force for ecosystem dynamics. J. Mar. Syst. 109-110, 78–93.

Dentener, F.J., Drevet, J., Lamarque, J.F., Bey, I., Eickhout, B., Fiore, A.M., Hauglustaine, D., Horowitz, L.W., Krol, M., Kulshrestha, U.C., Lawrance, M., Galy-Lacaux, C., Rast, S., Shindell, D., Stevenson, D., Van Noije, T., Atherton, C., Bell, N., Bergman, D., Butler, T., Cofala, J., Collins, B., Doherty, R., Ellingsen, K., Galloway, J., Gauss, M., Montarano, V., Muller, F.J., Pitari, G., Rodriguez, J., Sanderson, M., Solmon, F., Strahan, S., Schultz, M., Sudo, K., Szopa, S., Wild, O., 2006. Nitrogen and sulfur deposition on regional and global scales: a multi-model evaluation. Glob. Biogeochem. Cycles 20, GB4003. http://dx.doi.org/10.1029/2005GB002672. PP 21.

Driscoll, C.T., Whitall, D., Aber, J., Boyer, E., Castro, M., Cronan, C., Goodale, C.L., Groffman, P., Hopkinson, C., Lambert, K., Lawrence, G., Ollinger, S., 2003. Nitrogen pollution in the northeastern United States: sources, effects, and management options. BioScience 53, 357–374.

Duce, R.A., LaRoche, J., Altieri, K., Arrigo, K.R., Baker, A.R., Capone, D.G., Cornell, S., Dentener, F., Galloway, J., Ganeshram, R.S., Geider, R.J., Jickells, T., Kuypers, M.M., Langlois, R., Liss, P.S., Liu, S.M., Middelburg, J.J., Moore, C.M., Nickovic, S., Oschlies, A., Pedersen, T., Prospero, J., Schlitzer, R., Seitzinger, S., Sorensen, L.L., Uematsu, M., Ulloa, O., Voss, M., Ward, B., Zamora, L., 2008. Impacts of atmospheric anthropogenic nitrogen on the open ocean. Science 320, 893–897.

The European Monitoring and Evaluation Programme (EMEP), 2010. Transboundary Acidification, Eutrophication and Ground Level Ozone in Europe in 2008. EMEP Status Report 2010: July 21, 2010. http://webdab.emep.int/Unified_Model_Results/.

Erisman, J.W., Vermeulen, A., Hensen, A., Flechard, C., Dammgen, U., Fowler, D., Sutton, M., Grunhage, L., Tuovinen, J.-P., 2005. Monitoring and modeling of biosphere/atmosphere exchange of gases and aerosols in Europe. Environ. Pollut. 133, 403–413.

Flechard, C.R., Nemitz, E., Smith, R.I., Fowler, D., Vermeulen, A.T., Bleeker, A., Erisman, J.W., Simpson, D., Zhang, L., Tang, Y.S., Sutton, M.A., 2011. Dry deposition of reactive nitrogen to European ecosystems: a comparison of inferential models across the NitroEurope network. Atmos. Chem. Phys. 11, 2703–2728. http://dx.doi.org/10.5194/acp-11-2703-2011.

Foley, K.M., Roselle, S.J., Appel, K.W., Bhave, P.V., Pleim, J.E., Otte, T.L., Mathur, R., Sarwar, G., Young, O.J., Gilliam, C.G., Kelly, J.T., Gilland, A.B., Bash, J.O., 2010. Incremental testing of the Community Multiscale Air Quality (CMAQ) modeling system version 4.7. Geosci. Model Dev. 3, 205–226.

Fowler, D., et al., 2009. Atmospheric composition change: ecosystems–atmosphere interactions. Atmos. Environ. 43, 5193–5267.

Galloway, J.N., Townsend, A.R., Erisman, J.W., Bekunda, M., Cai, Z., Freney, J.R., Martinelli, L.A., Seitzinger, S.P., Sutton, M.A., 2008. Transformation of the nitrogen cycle: recent trends, questions, and potential solutions. Science 320, 889–892.

Geels, C., Hansen, K.M., Christensen, J.H., Ambelas Skjøth, C., Ellermann, T., Hedegaard, G.B., Hertel, O., Frohn, L.M., Gross, A., Brandt, J., 2012. Projected change in atmospheric nitrogen deposition to the Baltic Sea towards 2020. Atmos. Chem. Phys. 12, 2615–2629. http://dx.doi.org/10.5194/acp-12-2615-2012.

Holland, E.A., Braswell, B.H., Sulzman, J., Lamarque, J.-F., 2005. Nitrogen deposition onto the United States and western Europe: synthesis of observations and models. Ecol. Appl. 15 (1), 38–57.

Huneeus, N., Schulz, M., Balkanski, Y., Griesfeller, J., Prospero, J., Kinne, S., Bauer, S., Boucher, O., Chin, M., Dentener, F., Diehl, T., Easter, R., Fillmore, D., Ghan, S., Ginoux, P., Grini, A., Horowitz, L., Koch, D., Krol, M.C., Landing, W., Liu, X., Mahowald, N., Miller, R., Morcrette, J.-J., Myhre, G., Penner, J., Perlwitz, J., Stier, P., Takemura, T., Zender, C.S., 2011. Global dust model intercomparison in AeroCom phase I. Atmos. Chem. Phys. 11, 7781–7816.

Im, U., Markakis, K., Poupkou, A., Melas, D., Unal, A., Gerasopoulos, E., Daskalakis, N., Kindap, T., Kanakidou, M., 2011. The impact of temperature changes on summer time ozone and its precursors in the Eastern Mediterranean. Atmos. Chem. Phys. 11, 3847–3864.

Im, U., Markakis, K., Koçak, M., Gerasopoulos, E., Daskalakis, N., Mihalopoulos, N., Poupkou, A., Kindap, T., Unal, A., Kanakidou, M., 2012. Summertime aerosol chemical composition in the Eastern Mediterranean and its sensitivity to temperature. Atmos. Environ. 50, 164–173.

Im, U., Kanakidou, M., 2012. Impacts of East Mediterranean megacity emissions on air quality. Atmos. Chem. Phys. 12, 6335–6355.

Im, U., Daskalakis, N., Markakis, K., Vrekoussis, M., Hjorth, J., Myriokefalitakis, S., Gerasopoulos, E., Kouvarakis, G., Richter, A., Burrows, J., Pozzoli, L., Unal, A., Kindap, T., Kanakidou, M., 2013. Simulated air quality and pollutant budgets over Europe in 2008. Sci. Total Environ. http://dx.doi.org/10.1016/j.scitotenv.2013.09.090.

Kanakidou, M., Duce, R.A., Prospero, J.M., Baker, A.R., Benitez-Nelson, C., Dentener, F.J., Hunter, K.A.., Liss, P.S., Mahowald, N., Okin, G.S., Sarin, M., Tsigaridis, K., Uematsu, M., Zamora, L.M., Zhu, T., 2012. Atmospheric fluxes of organic N and P to the global ocean. Glob. Biogeochem. Cycles 26, GB3026. http://dx.doi.org/10.1029/2011GB004277, 12 PP.

Kocak, M., Kubilay, N., Tugrul, S., Mihalopoulos, N., 2010. Atmospheric nutrient inputs to the northern Levantine basin from a long-term observation: sources and comparisons with riverine inputs. Biogeosciences 7, 4037–4050.

Kouvarakis, G., Mihalopoulos, N., Tselepides, T., Stavrakakis, S., 2001. On the importance of atmospheric nitrogen inputs on the productivity of Eastern Mediterranean. Glob. Biogeochem. Cycles 15, 805–818.

Krom, M.D., Herut, B., Mantoura, R.F.C., 2004. Nutrient budget for the Eastern Mediterranean: implications for P limitation. Limnol. Oceanogr. 49, 1582–1592.

Lamarque, J.-F., Dentener, F., McConnell, J., Ro, C.-U., Shaw, M., Vet, R., Bergmann, D., Cameron-Smith, P., Dalsoren, S., Doherty, R., Faluvegi, G., Ghan, S.J., Josse, B., Lee, Y.H., MacKenzie, I.A., Plummer, D., Shindell, D.T., Skeie, R.B., Stevenson, D.S., Strode, S., Zeng, G., Curran, M., Dahl-Jensen, D., Das, S., Fritzsche, D., Nolan, M., 2013. Multi-model mean nitrogen and sulfur deposition from the Atmospheric Chemistry and Climate Model Intercomparison Project (ACCMIP): evaluation of historical and projected future changes. Atmos. Chem. Phys. 13, 7997–8018.

Ludwig, W., Dumont, E., Meybeck, M., Heussner, S., 2009. River discharges of water and nutrients to the Mediterranean and Black Sea: major drivers for ecosystem changes during the past and future decades? Prog. Oceanogr. 80, 199–217.
Markaki, Z., Loye-Pilot, M.D., Violaki, K., Benyahya, L., Mihalopoulos, N., 2010. Variability of atmospheric deposition of dissolved nitrogen and phosphorus in the Mediterranean and possible link to the anomalous seawater N/P ratio. Mar. Chem. 120, 187–194.
Matthias, V., Aulinger, A., Quante, M., 2008. Adapting CMAQ to investigate air pollution in North Sea coastal regions. Environ. Model. Softw. 23, 356–368.
Medinets, S., Medinets, V., 2012. Investigations of atmospheric wet and dry nutrient deposition to marine surface in western part of the Black Sea. Turk. J. Fish. Aquat. Sci. 12, 497–505.
Menegoz, M., Salas y Melia, D., Legrand, M., Teyssedre, H., Michou, M., Peuch, V.-H., Martet, M., Josse, B., Dombrowski-Etchevers, I., 2009. Equilibrium of sinks and sources of sulphate over Europe: comparison between a six-year simulation and EMEP observations. Atmos. Chem. Phys. 9, 4505–4519.
Mihalopoulos, N., Stephanou, E., Kanakidou, M., Pilitsidis, S., Bousquet, P., 1997. Tropospheric aerosol ionic composition in the Eastern Mediterranean region. Tellus 49B, 314–326.
Morales-Baquero, R., Pulido-Villena, E., Reche, I., 2006. Atmospheric inputs of phosphorus and nitrogen to southwest Mediterranean region: biogeochemical responses of high mountain lakes. Limnol. Oceanogr. 51 (2), 830–837.
Myriokefalitakis, S., Tsigaridis, K., Mihalopoulos, N., Sciare, J., Nenes, A., Kawamura, K., Segers, A., Kanakidou, M., 2011. In-cloud oxalate formation in the global troposphere: a 3-D modeling study. Atmos. Chem. Phys. 11, 5761–5782. http://dx.doi.org/10.5194/acpd-11-485-2011.
Otte, T.L., Pleim, J.E., 2010. The Meteorology-Chemistry Interface Processor (MCIP) for the CMAQ modeling system: updates through MCIPv3.4.1. Geosci. Model Dev. 3, 243–256.
Pleim, J., Xiu, A., Finkelstein, P.L., Otte, T.L., 2001. A coupled land-surface and dry deposition model and comparison to field measurements of surface heat, moisture, and ozone fluxes. Water Air Soil Pollut. Focus 1, 243–252.
Pozzer, A., de Meij, A., Pringle, K.J., Tost, H., Doering, U.M., van Aardanne, J., Lelieveld, J., 2012. Distributions and regional budgets of aerosols and their precursors simulated with the EMAC chemistry–climate model. Atmos. Chem. Phys. 12, 961–987.
Pryor, S.C., Gallagher, M., Sievering, H., Larsen, S.E., Barthelmie, R.J., Birsan, F., Nemitz, E., Rinne, J., Kulmala, M., Grönholm, T., Taipale, R., Vesala, T., 2008. A review of measurement and modelling results of particle atmosphere–surface exchange. Tellus 60, 42–75.
Redfield, A.C., 1934. On the proportions of organic derivations in sea water and their relation to the composition of plankton. In: Daniel, R.J. (Ed.), James Johnstone Memorial Volume. University Press of Liverpool, pp. 177–192.
Seinfeld, J.H., Pandis, S.N., 2006. Atmospheric Chemistry and Physics: from Air Pollution to Climate Change, third ed. John Wiley, New York.
Simpson, D., Butterbach-Bahl, K., Fagerli, H., Kesik, M., Skiba, U., Tang, S., 2006. Deposition and emissions of reactive nitrogen over European forests: a modeling study. Atmos. Environ. 40, 5712–5726.
Skamarock, W.C., Klemp, J.B., 2008. A time-split non-hydrostatic atmospheric model. J. Comput. Phys. 227, 3465–3485.
Ternon, E., Guieu, C., Loÿe-Pilot, M.-D., Leblond, N., Bosc, E., Gasser, B., Miquel, J.-C., Martín, J., 2010. The impact of Saharan dust on the particulate export in the water column of the North Western Mediterranean Sea. Biogeosciences 7, 809–826. http://dx.doi.org/10.5194/bg-7-809-2010.
Theodosi, C., Stavrakakis, S., Koulaki, F., Stavrakaki, I., Moncheva, S., Papathanasiou, E., Sanchez-Vidal, A., Kocak, M., Mihalopoulos, N., 2013. The significance of atmospheric inputs of major and trace metals to the Black Sea. J. Mar. Syst. 109–100, 94–102.
Tørseth, K., Aas, W., Breivik, K., Fjæraa, A.M., Fiebig, M., Hjellbrekke, A.G., Lund Myhre, C., Solberg, S., Yttri, K.E., 2012. Introduction to the European Monitoring and Evaluation Programme (EMEP) and observed atmospheric composition change during 1972–2009. Atmos. Chem. Phys. 12, 5447–5481.
United Nations, Economic Commission for Europe (UN-ECE), 2010. Empirical Critical Loads and Dose–Response Relationships (ECE/EB.AIR/WG.1/2010/14).
Violaki, K., Zarbas, P., Mihalopoulos, N., 2010. Long-term measurements of dissolved organic nitrogen (DON) in atmospheric deposition in the Eastern Mediterranean: fluxes, origin and biogeochemical implications. Mar. Chem. 120, 179–186.
Wesely, M.L., Hicks, B.B., 1977. Some factors that affect the deposition rates of sulfur dioxide and similar gases on vegetation. J. Air Pollut. Control Assoc. 27, 1110–1116.